DIFFUSE INTERFACE FORMULATIONS FOR REGION BASED ACTIVE CONTOUR IMAGE SEGMENTATION

Blaise Faugeras

LABORATOIRE

INFORMATIQUE, SIGNAUX ET SYSTÈMES
DE SOPHIA ANTIPOLIS
UMR 6070

DIFFUSE INTERFACE FORMULATIONS FOR REGION BASED ACTIVE CONTOUR IMAGE SEGMENTATION

Blaise Faugeras

Projet CREATIVE

Rapport de recherche
ISRN I3S/RR–2006-33–FR

Août 2006

LABORATOIRE I3S: Les Algorithmes / Euclide B – 2000 route des Lucioles – B.P. 121 –
06903 Sophia-Antipolis Cedex, France – Tél. (33) 492 942 701 – Télécopie : (33) 492 942 898
http://www.i3s.unice.fr/I3S/FR/

RÉSUMÉ :
Travail d'ingénieur de recherche supervisé par Eric Debreuve et Michel Barlaud.

MOTS CLÉS :

ABSTRACT:
Supervisors: Eric Debreuve and Michel Barlaud.

This paper investigates phase field models or diffuse interface formulations for region based active contour image segmentation. It was motivated by two earlier works: the use of a phase field model for higher-order active contours and a reformulation of the Mumford-Shah functional in terms of a diffuse interface model. Our main goal is to show how a diffuse interface formulation can advantageously be used for region competition segmentation.

KEY WORDS :
Phase field model, diffuse interface formulation, region-based segmentation, active contours

Diffuse interface formulations for region based active contour image segmentation

Blaise Faugeras - Equipe Creative

Août 2006

1 Introduction

This paper investigates phase field models or diffuse interface formulations for region based active contour image segmentation. It was motivated by [21] in which a phase field model for higher-order active contours is proposed and by [6] in which Mumford-Shah functional is reformulated in terms of a diffuse interface model. Our first goal is to show how a diffuse interface formulation can advantageously be used for region competition segmentation. In order to compare this formulation with existing ones let us first recall the classical procedure with which such a segmentation problem is dealt with.

Let $D \in \mathbf{R}^2$ be the domain of a given image whose intensity is represented by a function $I : D \to [0, M]$. In order to lighten notations through out the paper we consider that I is a scalar function, that is to say a gray-scale image. We will however also use color images in our numerical experiments.

The aim of image segmentation by region competition is to partition D in two sub-domains: Ω^+ the region of interest and Ω^-, its complement in D, the background region. They share the same boundary Γ. One usually looks for a region Ω^+ minimizing a functional combining region functionals and a regularization boundary functional:

$$E(\Omega^+) = \int_{\Omega^+} f(x, \Omega^+)dx + \int_{\Omega^-} f(x, \Omega^-)dx + \int_\Gamma \alpha ds \tag{1}$$

where f is a region-dependent descriptor. The minimization is performed using active contours. An initial curve Γ_0 is evolved with the equation

$$\partial_t \Gamma(s, t) = v(s, t)n(s, t)$$

where s is the arc length, t the time evolution parameter, v is the velocity and n is a vector normal to $\Gamma(s, t)$ (directed from Ω^- to Ω^+). A difficulty is to compute the velocity from the energy E and a nice way to do this is to use shape derivation methods as detailed in [3, 14].

Once the velocity v is computed it remains to implement an active contour numerical procedure. A first approach is to parameterize explicitly the contour using polygons or splines for example. This is the snake method (eg. [15, 20]). The main drawback of this representation is that topological changes are difficult

to handle. The level set method [19, 24] is a second approach in which the contour is represented implicitly as the zero level set of a function. With a level set function contours may break or merge automatically during the evolution. However another difficulty rises. Numerically it is necessary to keep the evolving level set function close to a signed distance function to Γ. The traditional way to deal with this is to periodically re-initialize the level set function to a signed distance function. From a practical point of view this is expensive and not easily implemented. From a theoretical point of view it is not completely satisfactory [10, 17].

In [21] the authors were concerned the problem of the extraction of line networks from remote sensing images and advertise that phase field models offer a good alternative to classical active contour methods. Phase field models originate from the study of moving boundary problems in physics. A simple model is given by the Allen-Cahn reaction-diffusion equation [1].

$$\partial_t \phi = \Delta \phi - \frac{1}{\varepsilon^2} V'(\phi)$$

where V' is the derivative of a smooth double equal well potential V with minima at ± 1. The main feature of the solution to this equation is that it separates the domain in two subdomains (or phases in which $\phi = \pm 1$) and the motion of its zero level set at the diffuse interface approximates motion by mean curvature when ε is small (eg. [22, 7]).

Phase field models provide an interesting way to model regions or phases and their moving boundaries. The possibility to use them in image science has been very little explored. We found the recent papers [25, 6] and [21] in which [23, 2, 11] were cited. In this study we propose two phase field models and numerical methods for region based active contour segmentation. We focus on two specific descriptors: the mean descriptor and the entropy descriptor. The mean descriptor is well known (eg. [4, 5]) and reads:

$$f(x, \Omega^{\pm}) = (I(x) - \mu(\Omega^{\pm}))^2 \tag{2}$$

where $\mu(\Omega^{\pm})$ represents the mean of the intensity over region $\Omega^{\pm}$ computed as

$$\mu(\Omega^{\pm}) = \frac{1}{|\Omega^{\pm}|} \int_{\Omega^{\pm}} I(x) dx \tag{3}$$

The entropy descriptor is less classic but proved to be efficient for image segmentation [16, 12, 13]. Let us define

$$f(x, \Omega^{\pm}) = k(\Omega^{\pm}) = \int_{\mathbf{R}} -p(i, \Omega^{\pm}) \ln(p(i, \Omega^{\pm})) di \tag{4}$$

where the probability density distributions, $p(i, \Omega^{\pm})$, of the random variables whose samples are the values of the intensity I in $\Omega^{\pm}$ are estimated using the Parzen window method

$$p(i, \Omega^{\pm}) = \frac{1}{|\Omega^{\pm}|} \int_{\Omega^{\pm}} K(I(x) - i) dx \tag{5}$$

and K is a 0-mean Gaussian kernel.

The remaining part of the paper is organized as follows. A diffuse interface formulation for segmentation using these two descriptors is given in Section 2. In Section 3 we conduct an asymptotic analysis of the model and obtain an approximation of the velocity of the interface. This clarifies the link between classical active contours and phase field formulations since the derived approximation is similar to the expression of the velocity obtained in the region based framework of Eq. (1): shape differentiation leads to the following expression for the normal velocity of the active contour in the mean descriptor case

$$v(s,t) = (I(s) - \mu(\Omega^+)(t))^2 - (I(s) - \mu(\Omega^-)(t))^2 + \alpha\kappa(s,t) \tag{6}$$

where κ is the curvature of Γ, and in the entropy descriptor case

$$v(s,t) = \int_{\mathbf{R}} (\ln(p(i,\Omega^-))(t) - \ln(p(i,\Omega^+))(t))K(I(s) - i)di + \alpha\kappa(s,t) \tag{7}$$

Section 4 deals with the numerical implementation of the model. Two schemes based on operator splitting methods are proposed and compared. Several segmentation experiments are conducted in the end and illustrate the method.

2 Phase field formulation

In this section we formulate the energy which will be minimized in order to segment an image I. The energy is expressed in terms of a phase field that is to say a function $\phi : D \to \mathbf{R}$. The phase field framework for image segmentation is a level set framework since we seek ϕ such that

$$\begin{cases} \phi(x) > 0 \text{ and } \phi(x) \approx 1 \text{ if } x \in \Omega^+ \\ \phi(x) < 0 \text{ and } \phi(x) \approx -1 \text{ if } x \in \Omega^- \end{cases} \tag{8}$$

and the contour Γ is described implicitly by $\Gamma = \{x \in D, \phi(x) = 0\}$.

2.1 Energy

The phase field is sought as the optimal function minimizing an energy $E(\phi)$ which is the sum of a diffuse interface energy, $E_p(\phi)$ and a segmentation energy $E_s(\phi)$.

Diffuse interface energy The diffuse interface energy is defined as

$$E_p(\phi) = \int_D \frac{d}{2}||\nabla\phi(x)||^2 + \frac{1}{\varepsilon^2}V(\phi(x))dx \tag{9}$$

where $V(s) = \frac{1}{4}(1 - s^2)^2$ is the classical quartic double well potential, with minima at ± 1. The parameter ε is small and strictly positive and a bounded energy will therefore force $\phi = 1$ or $\phi = -1$ almost everywhere. The gradient term prevents any discontinuity to occur at the interface between the two phases and the diffusion parameter $d > 0$ controls the smoothness of the transition.

Segmentation energy We now come to the segmentation part of the energy functional. Using ϕ we rewrite Eq. (1) dropping the regularization term which arises from the diffuse interface energy term as it is shown in Section 3.

Since $\phi \approx \pm 1$ the indicator functions for regions $\Omega^{\pm}$ are given in first approximation by

$$\mathbb{1}_{\Omega^+}(x) = \left(\frac{1+\phi(x)}{2}\right)^2 \tag{10}$$

$$\mathbb{1}_{\Omega^-(x)} = \left(\frac{1-\phi(x)}{2}\right)^2 \tag{11}$$

The only reason for the square is computational stability. It guarantees that the indicator functions stay positive even if extreme values of ϕ are not exactly ± 1.

The segmentation can be written in a general form as

$$E_s(\phi) = \int_D \left(\frac{1+\phi(x)}{2}\right)^2 k_{\Omega^+}(x,\phi)dx + \int_D \left(\frac{1-\phi(x)}{2}\right)^2 k_{\Omega^-}(x,\phi)dx \tag{12}$$

Let us explicit the different terms in both the mean descriptor case and the entropy descriptor case which we focus on.

Mean descriptor Rewriting Eqs. (3) and (2) in terms of ϕ yields:

$$\mu_{\Omega^\pm}(\phi) = \frac{1}{\displaystyle\int_D \left(\frac{1\pm\phi(x)}{2}\right)^2 dx} \int_D \left(\frac{1\pm\phi(x)}{2}\right)^2 I(x)dx \tag{13}$$

and

$$\begin{aligned} E_s(\phi) \quad &= \int_D \left(\frac{1+\phi(x)}{2}\right)^2 (I(x)-\mu_{\Omega^+}(\phi))^2 dx \\ &+ \int_D \left(\frac{1-\phi(x)}{2}\right)^2 (I(x)-\mu_{\Omega^-}(\phi))^2 dx \end{aligned} \tag{14}$$

for the segmentation energy.

Entropy descriptor Similarly rewriting Eqs. (5) and (4) in terms of ϕ gives

$$p_{\Omega^\pm}(i,\phi) = \frac{1}{\displaystyle\int_D (\frac{1\pm\phi(x)}{2})^2 dx} \int_D (\frac{1\pm\phi(x)}{2})^2 K(I(x)-i)dx \tag{15}$$

for the probability density distribution and the segmentation energy is finally given by

$$\begin{aligned} E_s(\phi) \quad &= \int_D (\frac{1+\phi(x)}{2})^2 dx \int_{\mathbf{R}} -p_{\Omega^+}(i,\phi)\ln(p_{\Omega^+}(i,\phi))di \\ &+ \int_D (\frac{1-\phi(x)}{2})^2 dx \int_{\mathbf{R}} -p_{\Omega^-}(i,\phi)\ln(p_{\Omega^-}(i,\phi))di \end{aligned} \tag{16}$$

2.2 Minimization

Let us now derive the non-linear, non-local parabolic equations which are solved both in the mean descriptor case and in the entropy descriptor case to minimize the energy E whose final expression is

$$E(\phi) = E_p(\phi) + \frac{w}{\varepsilon} E_s(\phi) \tag{17}$$

where w is weighting parameter. The reason for introducing a $1/\varepsilon$ factor comes from the asymptotic analysis of Section 3.

The Euler-Lagrange equation for the unknown function ϕ is computed from the directional derivative, $E'(\phi;\psi)$ of E at point $\phi \in L^2(D)$ in direction $\psi \in L^2(D)$.

For E_p we obtain in a straight forward manner

$$\begin{aligned} E'_p(\phi;\psi) &= \int_D d\nabla\phi(x).\nabla\psi(x) + \frac{1}{\varepsilon^2}V'(\phi(x))\psi(x)dx \\ &= \int_D -d\Delta\phi(x)\psi(x)dx + \int_{\partial D} d\nabla\phi.n\psi ds + \frac{1}{\varepsilon^2}V'(\phi(x))\psi(x)dx \end{aligned} \tag{18}$$

We now deal with the segmentation terms.

Mean descriptor After some calculations we obtain

$$E'_s(\phi;\psi) = \int_D [(\frac{1+\phi(x)}{2})(I(x)-\mu_{\Omega^+}(\phi))^2 - (\frac{1-\phi(x)}{2})(I(x)-\mu_{\Omega^-}(\phi))^2]\psi(x)dx \tag{19}$$

The Euler-Lagrange equation for the complete energy then reads

$$E'(\phi;\psi) = 0 \ \forall\psi \tag{20}$$

which can be written as a boundary value problem

$$\begin{cases} -d\Delta\phi(x) + \frac{1}{\varepsilon^2}V'(\phi(x)) & \\ +\frac{w}{\varepsilon}[(\frac{1+\phi(x)}{2})(I(x)-\mu_{\Omega^+}(\phi))^2 - (\frac{1-\phi(x)}{2})(I(x)-\mu_{\Omega^-}(\phi))^2] = 0 & \text{in } D, \\ \nabla\phi.n = 0 & \text{in } \partial D \end{cases} \tag{21}$$

A common approach we follow to solve such a minimization problem is to perform a gradient descent which consists in solving the following gradient flow initial boundary value problem to steady state

$$\begin{cases} \partial_t\phi(x,t) = d\Delta\phi(x,t) - \frac{1}{\varepsilon^2}V'(\phi(x,t)) & \\ -\frac{w}{\varepsilon}[(\frac{1+\phi(x,t)}{2})(I(x)-\mu_{\Omega^+}(\phi))^2 & \\ -(\frac{1-\phi(x,t)}{2})(I(x)-\mu_{\Omega^-}(\phi))^2] & \text{in } D\times(0,T), \\ \nabla\phi.n = 0 & \text{in } \partial D\times(0,T) \\ \phi(x,0) = \phi^0(x) & \text{in } D \end{cases} \tag{22}$$

Entropy descriptor After some calculations we derive

$$\begin{aligned} E'_s(\phi,\psi) &= \int_D (\frac{1+\phi(x)}{2})[\int_{\mathbf{R}} -\ln(p_{\Omega^+}(i,\phi))K(I(x)-i)di] \\ &\quad -(\frac{1-\phi(x)}{2})[\int_{\mathbf{R}} -\ln(p_{\Omega^-}(i,\phi))K(I(x)-i)di]\psi(x)dx \end{aligned} \tag{23}$$

and the associated gradient flow initial boundary value problem reads:

$$\begin{cases} \partial_t\phi(x,t) = d\Delta\phi(x,t) - \dfrac{1}{\varepsilon^2}V'(\phi(x,t)) \\ -\dfrac{w}{\varepsilon}\{(\dfrac{1+\phi(x,t)}{2})[\displaystyle\int_{\mathbf{R}} -\ln(p_{\Omega^+}(i,\phi))K(I(x)-i)di] \\ -(\dfrac{1-\phi(x,t)}{2})[\displaystyle\int_{\mathbf{R}} -\ln(p_{\Omega^-}(i,\phi))K(I(x)-i)di]\} & \text{in } D\times(0,T), \\ \nabla\phi.n = 0 & \text{in } \partial D\times(0,T) \\ \phi(x,0) = \phi^0(x) & \text{in } D \end{cases} \tag{24}$$

3 Asymptotic analysis

In this section we adapt a formal asymptotic analysis method developed for phase field models [8, 9] and provide an approximation of the normal velocity of the moving interface $\Gamma(t) = \{x \in D, \phi(x,t) = 0\}$. The derived approximation is similar to the expression obtained in the region based framework using shape differentiation.

Let us consider the nonlocal ε-dependent equation

$$\varepsilon^2\partial_t\phi^\varepsilon(x,t) = \varepsilon^2 d\Delta\phi^\varepsilon(x,t) - V'(\phi^\varepsilon(x,t)) - \varepsilon S(\phi^\varepsilon(x,t),\phi^\varepsilon) \tag{25}$$

The superscript ε indicates that we consider a family of solutions as $\varepsilon \to 0$.

The segmentation energy term, S, which has a local and a non local dependence on ϕ^ε can be written in both the mean descriptor and the entropy case as

$$S(\phi^\varepsilon(x,t),\phi^\varepsilon) = S_1(\phi^\varepsilon) + \phi^\varepsilon(x,t)S_2(\phi^\varepsilon) \tag{26}$$

where S_1 and S_2 are non-local functions of ϕ^ε. The analysis consists in considering an outer expansion in powers of ε, valid in regions away from the interface $\Gamma^\varepsilon(t)$ and also an inner expansion valid near $\Gamma^\varepsilon(t)$.

Outer solution In the outer region let us consider the expansion

$$\phi^\varepsilon(x,t) = \phi_0(x,t) + \varepsilon\phi_1(x,t) + \varepsilon^2\phi_2(x,t)\dots \tag{27}$$

Inserting it into Eq. (25) leads to

$$V'(\phi_0(x,t)) + \mathcal{O}(\varepsilon) = 0 \tag{28}$$

and therefore

$$\phi_0(x,t) = \pm 1 \tag{29}$$

Assume that $\Gamma^\varepsilon(t)$ separates D into two regions $\Omega^\varepsilon_\pm$ and let us select the outer solution so that

$$\phi_0(x,t) = \begin{cases} +1 & \text{if } x \in \Omega^0_+(t), \\ -1 & \text{if } x \in \Omega^0_-(t). \end{cases} \tag{30}$$

From now on we assume that the nonlocal part of the segmentation term satisfies

$$S(\phi^\varepsilon(x,t), \phi^\varepsilon) = S(\phi^\varepsilon(x,t), \phi_0) + \mathcal{O}(\varepsilon) \tag{31}$$

Inner solution In the inner region a local orthogonal coordinate system (r,s) defined in a neighborhood of $\Gamma^\varepsilon(t)$ is used where r is the signed distance from x to $\Gamma^\varepsilon(t)$ and s is the distance along the interface. The coordinate system is oriented so that $r > 0$ corresponds to $\phi > 0$. Let us define the scaled normal coordinate $\rho = r/\varepsilon$, $\Phi^\varepsilon(\rho,s,t) = \phi^\varepsilon(x,t)$ and the formal expansion

$$\Phi^\varepsilon(\rho,s,t) = \Phi_0(\rho,s,t) + \varepsilon\Phi_1(\rho,s,t) + \varepsilon^2\Phi_2(\rho,s,t)\dots \tag{32}$$

Quantities which depend on the zero level set Γ^ε, such as the normal velocity, v^ε, and the curvature κ^ε, also require the same expansion. In the new coordinate system Eq. (25) takes the form

$$d\partial^2_\rho\Phi^\varepsilon - V'(\Phi^\varepsilon) + \varepsilon(d\Delta r\partial_\rho\Phi^\varepsilon - \partial_t r\partial_\rho\Phi^\varepsilon - S(\Phi^\varepsilon,\phi^\varepsilon)) + \mathcal{O}(\varepsilon^2) = 0 \tag{33}$$

With the convention that a convex region of $\phi > 0$ has positive curvature and that the normal velocity of the interface is postive when it moves positively in the r coordinate. From $\Delta r = -\kappa_0 + \mathcal{O}(\varepsilon)$, $\partial_t r = -v_0 + \mathcal{O}(\varepsilon)$ and Eq. (31) we obtain

$$d\partial^2_\rho\Phi_0 - V'(\Phi_0) + \varepsilon(d\partial^2_\rho\Phi_1 - V''(\Phi_0)\Phi_1 - d\kappa_0\partial_\rho\Phi_0 + v_0\partial_\rho\Phi_0 - S(\Phi_0,\phi_0)) + \mathcal{O}(\varepsilon^2) = 0 \tag{34}$$

- $\mathcal{O}(1)$ **term:** Φ_0 satisfies

  $$d\partial^2_\rho\Phi_0 - V'(\Phi_0) = 0 \tag{35}$$

  Moreover, the inner and outer expansions must describe the same solution in an intermediate zone where $\varepsilon \ll |r| \ll 1$ or $1 \ll |\rho| \ll 1/\varepsilon$. This gives the matching conditions

  $$\lim_{\rho\to\pm\infty} \Phi_0(\rho,s,t) = \pm 1 \tag{36}$$

  Eq. (35) with boundary conditions (36) integrates to

  $$\Phi_0(\rho,s,t) = \Phi_0(\rho) = \tanh(\frac{\rho}{\sqrt{d}}) \tag{37}$$

  which is the profile of the transition layer.

- $\mathcal{O}(\varepsilon)$ **term:** We obtain the equation

  $$[d\partial^2_\rho . - V''(\Phi_0)]\Phi_1 = -(v_0 - d\kappa_0)\Phi_0' + S(\Phi_0,\phi_0) \tag{38}$$

  This linear equation only has solutions when the right hand side is orthogonal to functions in the kernel of the operator which appears on the left

hand side. Differentiating Eq. (35) shows that Φ_0' is in the kernel. The solvability condition is then obtained by multiplying Eq. (38) by Φ_0' and integrating over ρ from $-\infty$ to ∞

$$\begin{aligned} 0 = \quad & S_1(\phi_0)(t) \int_{-\infty}^{\infty} \Phi_0'(\rho) d\rho + S_2(\phi_0)(t) \int_{-\infty}^{\infty} \Phi_0(\rho)\Phi_0'(\rho) d\rho \\ & -(v_0(s,t) - d\kappa_0(s,t)) \int_{-\infty}^{\infty} (\Phi_0'(\rho))^2 d\rho \end{aligned} \tag{39}$$

This equation gives the following expression for the velocity of the interface

$$v_0(s,t) = d\kappa_0(s,t) + \frac{3\sqrt{d}}{2} S_1(\phi_0)(t) \tag{40}$$

In the mean descriptor case, Eq. (40) becomes

$$v_0(s,t) = d\kappa_0(s,t) + \frac{3w\sqrt{d}}{4}(I(s) - \mu_{\Omega^+}(\phi_0)(t))^2 - (I(s) - \mu_{\Omega^-}(\phi_0)(t))^2 \tag{41}$$

and the entropy descriptor case

$$v_0(s,t) = d\kappa_0(s,t) + \frac{3w\sqrt{d}}{4}\left(\int_{\mathbf{R}} (\ln(p_{\Omega^-}(i,\phi))(t) - \ln(p_{\Omega^+}(i,\phi))(t)) K(I(s) - i) di\right) \tag{42}$$

Two points are worth noticing to conclude this section:

- As expected Eq. (41) is similar to Eq. (6) obtained with the shape gradient method. The same remark holds in the case of the entropy descriptor for Eqs. (42) and (7).
- The diffusion coefficient d appears as a weighting parameter for the curvature term which is not surprising since it was introduced to modulate the smoothing effect of diffusion. More surprisingly it also appears before the segmentation term.

4 Numerical implementation and experiments

4.1 First scheme

Let us give a first approximation procedure of the model. A finite difference discretization combined with an operator splitting method is used to solve the initial boundary value problem (43).

$$\begin{cases} \partial_t \phi(x,t) = d\Delta\phi(x,t) - \dfrac{1}{\varepsilon^2} V'(\phi(x,t)) - \dfrac{1}{\varepsilon} S(\phi(x,t),\phi) & \text{in } D \times (0,T), \\ \nabla\phi.n = 0 & \text{in } \partial D \times (0,T) \\ \phi(x,0) = \phi^0(x) & \text{in } D \end{cases} \tag{43}$$

The domain D is given as $(0, D_x) \times (0, D_y)$. Let h denote the spatial step in both the x and y direction and Δt the time step. The discretization points

are denoted by (x_i, y_j, t_n) with $i \in [1:I]$, $j \in [1:J]$ and $n \in [1:N]$. In what follows ϕ^n denotes an approximation of $\phi(x, y, t_n)$ and ϕ^n_{ij} and approximation of $\phi(x_i, y_j, t_n)$.

Algorithm 1 The operator splitting method we propose to solve problem (43) is the following. At each time step, given an approximation ϕ^n the computation of ϕ^{n+1} from ϕ^n is achieved in three steps.

Step 1. The linear diffusion equation in the x variable is integrated on $[t^n, t^{n+1}]$.

$$\begin{cases} \partial_t \phi(x,y,t) = d\partial_x^2 \phi(x,y,t) & \text{in } (0,D_x) \times (t^n, t^{n+1}),\ \forall y \in (0,D_y) \\ \partial_x \phi(0,y,t) = \partial_x \phi(D_x,y,t) = 0 & \text{in } (t^n, t^{n+1}),\ \forall y \in (0,D_y) \\ \phi(x,y,t^n) = \phi^n & \text{in } D \end{cases} \tag{44}$$

It results in a first approximation $\phi^{n+1,1}$. This step is conducted using an implicit scheme which guarantees stability. Let A be the classical $I \times I$ tridiagonal matrix defined by

$$A = \begin{pmatrix} 1+\alpha & -\alpha & & & \\ -\alpha & 1+2\alpha & -\alpha & & \\ & \ddots & \ddots & \ddots & \\ & & -\alpha & 1+2\alpha & -\alpha \\ & & & -\alpha & 1+\alpha \end{pmatrix} \tag{45}$$

with $\alpha = \dfrac{d\Delta t}{\Delta x^2}$, then solve the J linear systems

$$A\phi_j^{n+1,1} = \phi_j^n \tag{46}$$

with $\phi_j^n = (\phi_{1j}^n, \dots\ ,\ \phi_{Ij}^n)^T$

Step 2. The linear diffusion equation in the y variable is integrated in the same way in a second step on $[t^n, t^{n+1}]$ starting from $\phi^{n+1,1}$

$$\begin{cases} \partial_t \phi(x,y,t) = d\partial_y^2 \phi(x,y,t) & \text{in } (0,D_y) \times (t^n, t^{n+1}),\ \forall x \in (0,D_x) \\ \partial_y \phi(x,0,t) = \partial_y \phi(x,D_y,t) = 0 & \text{in } (t^n, t^{n+1}),\ \forall x \in (0,D_x) \\ \phi(x,y,t^n) = \phi^{n+1,1} & \text{in } D \end{cases} \tag{47}$$

It results in a second approximation $\phi^{n+1,2}$.

Step 3. The nonlinear reaction terms are integrated on $[t^n, t^{n+1}]$

$$\begin{cases} \partial_t \phi(x,y,t) = -\dfrac{1}{\varepsilon^2} V'(\phi(x,y,t)) - \dfrac{w}{\varepsilon} S(\phi(x,y,t), \phi) \\ \phi(x,y,t^n) = \phi^{n+1,2} \end{cases} \tag{48}$$

It results in the final value ϕ^{n+1}. This step is conducted using a simple explicit Euler method.

$$\phi_{i,j}^{n+1,1} = \phi_{i,j}^n - \Delta t \left(\frac{1}{\varepsilon^2} V'(\phi_{i,j}^n) + \frac{w}{\varepsilon} S(\phi_{i,j}^n, \phi^n),\ \forall i,j \right. \tag{49}$$

The integrals in $S(\phi_{i,j}^n, \phi^n)$ are evaluated as simple sums.

4.2 A second scheme

The main drawback of the previous scheme is that since ε cannot be chosen infinitely small the phase field values are not exactly ± 1 in the regions $\Omega^{\pm}$. This might cause numerical problems in the computation of the integrals of the segmentation terms (even though we chose the indicator functions of regions $\Omega^{\pm}$ to be defined as $(\frac{1\pm\phi}{2})^2$ and not simply $\frac{1\pm\phi}{2}$). Moreover to prevent the algorithm from diverging and the phase field from going to far away from ± 1 a relatively small time step has to be selected.

In this section we propose a second scheme which proves to be quite efficient. The ideas for this scheme come from the MBO scheme of [18] introduced to approximate the motion of an interface by its mean curvature and from [6] where the authors derive formal threshold dynamics for an initial boundary value problem similar to the one obtained in our mean descriptor case.

The MBO scheme can be interpreted as a splitting method for the Allen-Cahn equation,

$$\partial_t \phi = \Delta \phi - \frac{1}{\varepsilon^2} V'(\phi)$$

in which the step solving the ODE

$$\partial_t \phi = -\frac{1}{\varepsilon^2} V'(\phi) \text{ on } [t^n, t^{n+1}]$$

is turned into a thresholding step. It is supposed that at every point x the value of $\phi(x,t)$ converges very rapidly to one of the two stables equilibrium values ± 1, depending on whose basin of attraction it initially lies in.

Our second algorithm is an operator splitting scheme with two time steps and in which contrary to the first algorithm we first group together the diffusion and the segmentation terms and split the phasefield potential term apart. We suppose $\varepsilon^2 \ll \varepsilon \ll 1$ and threshold the potential term but not the segmentation one.

Thanks to this thresholding step ϕ always stays close to the values ± 1 and we can simply define the indicator functions of regions $\Omega^{\pm}$ as $\frac{1\pm\phi}{2}$. This simplifies the segmentation terms which become

$$S(\phi) = -\frac{w}{2}[(I(x) - \mu_{\Omega^+}(\phi))^2 - (I(x) - \mu_{\Omega^-}(\phi))^2]$$

in the mean descriptor case and

$$S(\phi) = -\frac{w}{2} \int_{\mathbf{R}} (\ln(p_{\Omega^-}(i,\phi)) - \ln(p_{\Omega^+}(i,\phi))) K(I(x) - i) di$$

in the entropy descriptor case. The asymptotic analysis of Section 3 remains valid with this formulation taking $S_2 \equiv 0$.

Algorithm 2 The algorithm reads as follows

Step 1. Integrate from t^n to $t^{n+1} = t^n + \Delta t$

$$\begin{cases} \partial_t \phi(x,y,t) = d\Delta\phi(x,y,t) + \dfrac{1}{\varepsilon} S(\phi) & \text{in } D \times (t^n, t^{n+1}), \\ \nabla\phi.n = 0 & \text{in } (t^n, t^{n+1}) \times \partial D \\ \phi(x,y,t^n) = \phi^n & \text{in } D \end{cases} \tag{50}$$

using the splitting of the first algorithm and a sub time step $\Delta t' = \frac{\Delta t}{k}$. It results in a first approximation $\phi^{n+1,1}$.

Step 2. Integrate the phasefield potential term on $[t^n, t^{n+1}]$ by thresholding

$$\phi^{n+1} = \begin{cases} +1 & \text{if } \phi_{ij}^{n+1,1} \geq 0 \\ -1 & \text{if } \phi_{ij}^{n+1,1} < 0 \end{cases} \tag{51}$$

It results in the final approximation ϕ^{n+1}.

4.3 Numerical results

In this section we illustrate Algorithm1 and 2 using either the mean descriptor or the entropy descriptor. We use two real images: a 512×512 grayscale bone medical image and a 288×352 color image drawn from the video sequence *Erik*.

In all experiments presented below we chose $h = 0.1$. In order to resolve the diffuse transition layer one should choose $\varepsilon \gg h$. We chose $\varepsilon = 5h$. The time step is $\Delta t = 0.1$. Concerning the diffusion coefficient d which controls the smoothness of the interface, small values enable the segmentation algorithm to capture many details while higher values result in smooth objects. We selected $d = 5$. The only parameter remaining to be tuned is the weight w whose value depends on the experiment. In order to use approximately the same weights w while using the mean or the entropy descriptor we chose to rescale the image intensity I to $[-1\ 1]$ in the mean descriptor case.

As mentioned in [21] a major advantage of phase field formulations is that the initial phase field can be chosen neutrally. We use $\phi^0 = 0 + \eta$ where η is a small white noise. More traditionally an initial contour Γ^0 can also be defined. We then set $\phi^0 = \pm 1$ in $\Omega^{\pm}$.

The algorithm stops when the slope of the decreasing segmentation energy, $t \mapsto E_s(\phi)(t)$ is lower than a small threshold value.

Figures ... make a selection ...

Algo 2 is more stable and faster

5 Conclusion

We have proposed two phase field models or diffuse interface formulations based on two descriptors for region-based active contour segmentation. They consist in a family of initial boundary value problems defined on the domain of the image and depending on a small parameter ε.

We have performed a formal asymptotic analysis of the models as $\varepsilon \to 0$ and obtained an approximation of the velocity of the diffuse interface. This approximation appeared to be similar to the expression of the velocity obtained in the region based framework using shape differentiation tools. This clarified the link between the phase field methodology to evolve contours for image segmentation with the classical approaches: snakes and level sets.

Eventually we proposed two algorithms based on operator splitting to solve the initial boundary value problems. The second one proved to be very efficient, much more stable and faster than the first one.

This study reenforces the conclusions of [21]: phase field models offer an advantageous alternative to classical active contour methods.

Future: non smooth double obstacle potential?

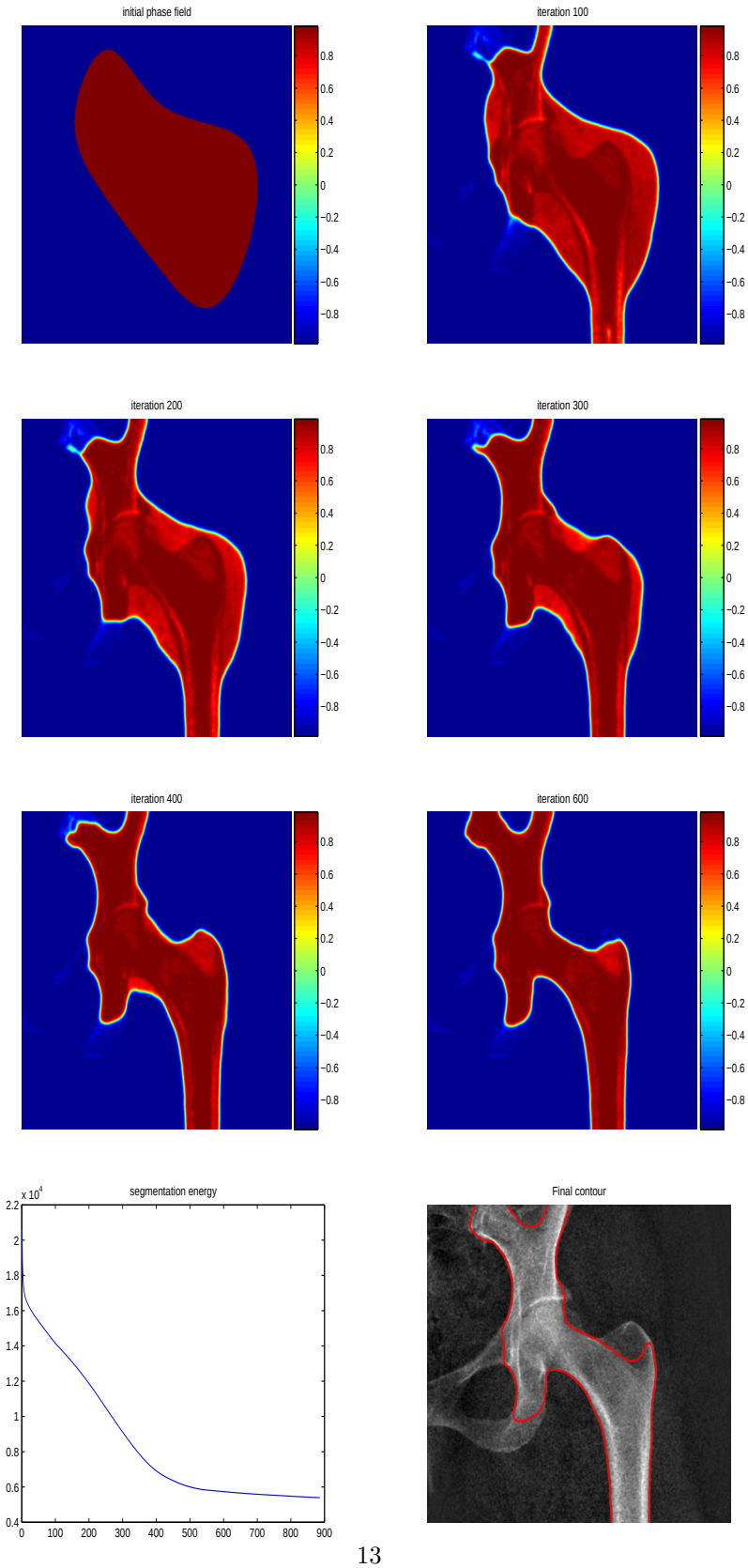

Figure 1: Segmentation of the femur image using the mean descriptor, an initial contour and algorithm 1. Last row, left: variations of the energy as a function of the number of iterations.

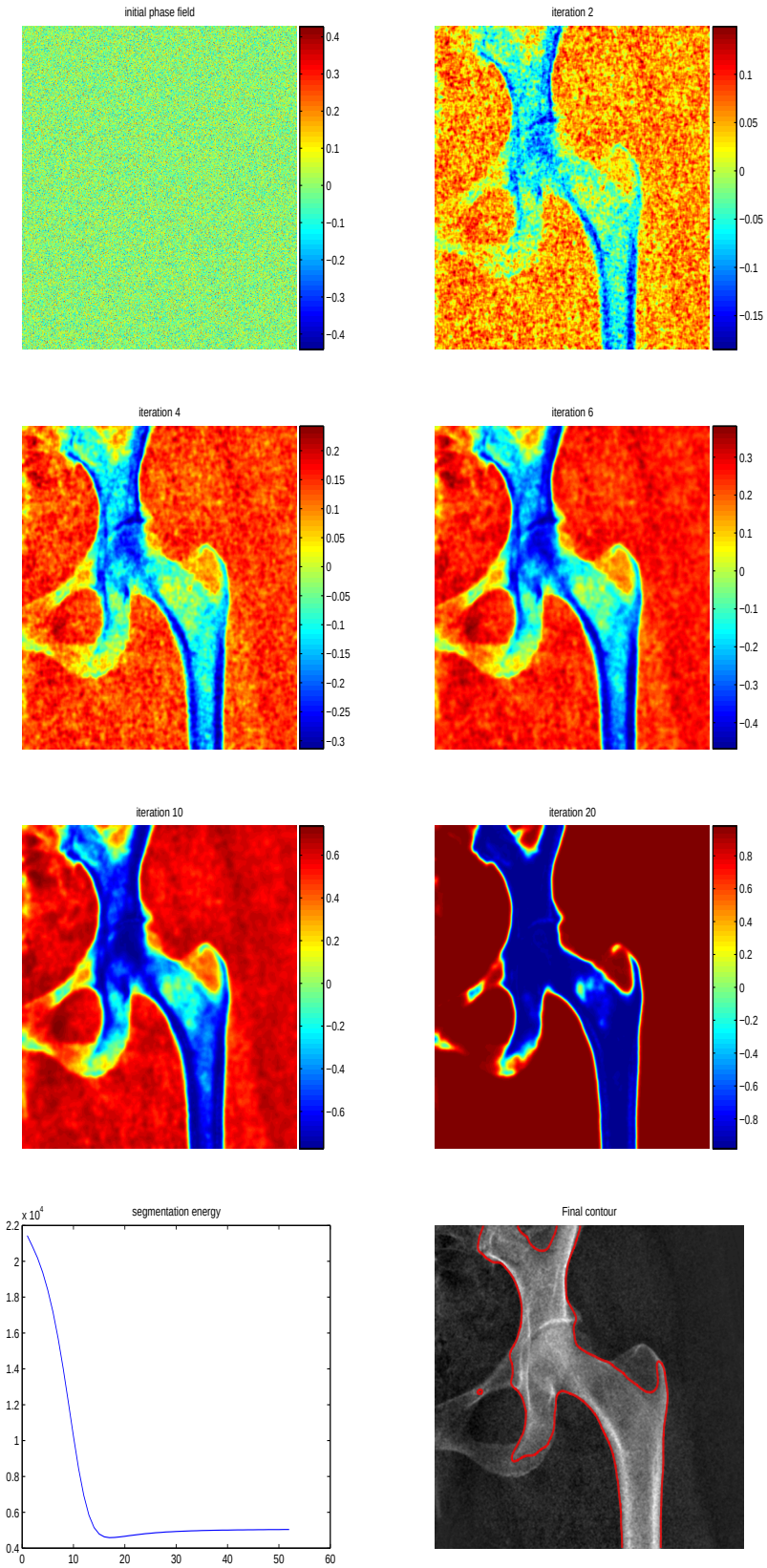

Figure 2: Segmentation of the femur image using the mean descriptor, a random initialization and algorithm 1. Last row, left: variations of the energy as a function of the number of iterations.

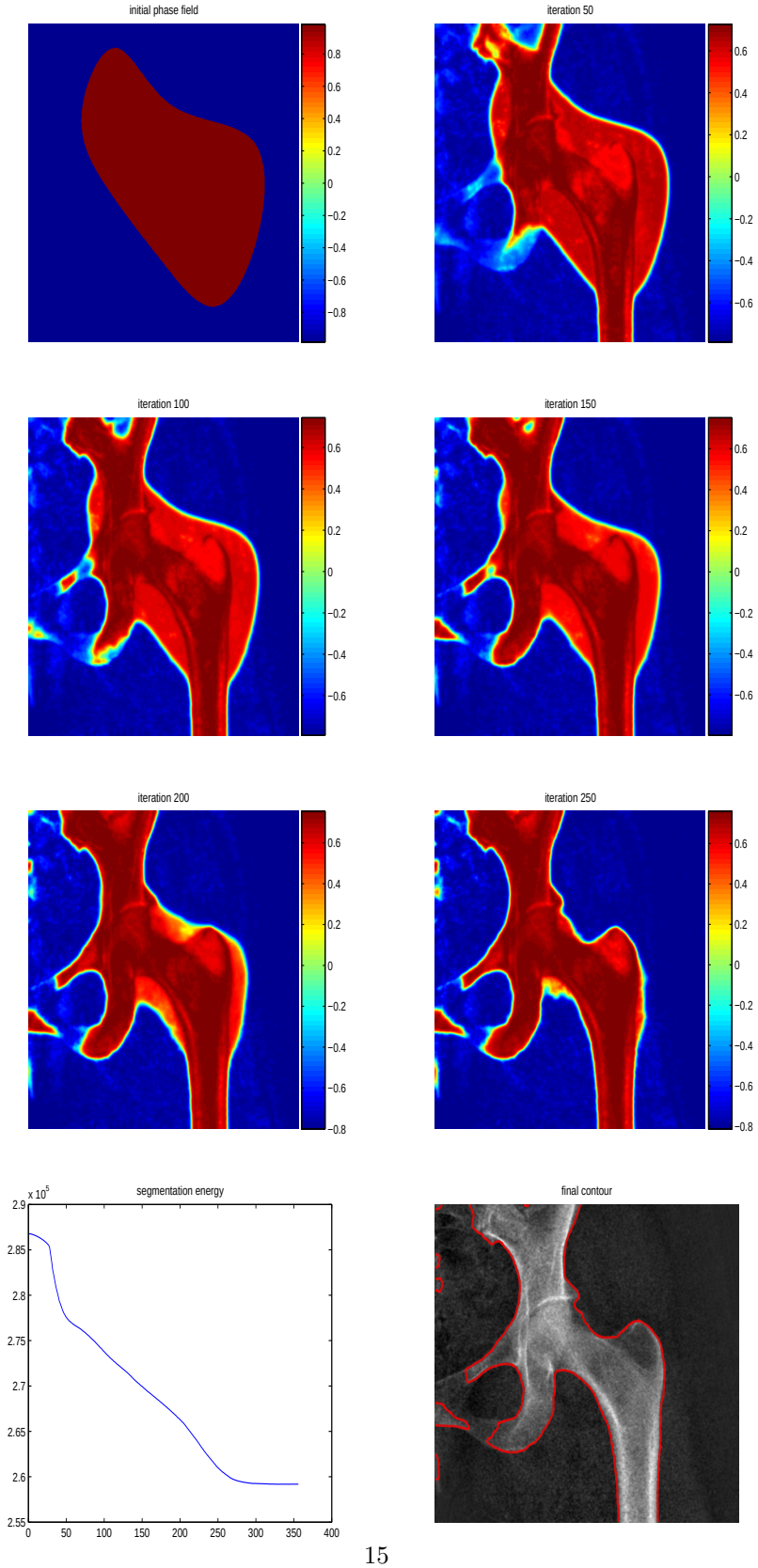

Figure 3: Segmentation of the femur image using the entropy descriptor, an initial contour and algorithm 1. Last row, left: variations of the energy as a function of the number of iterations.

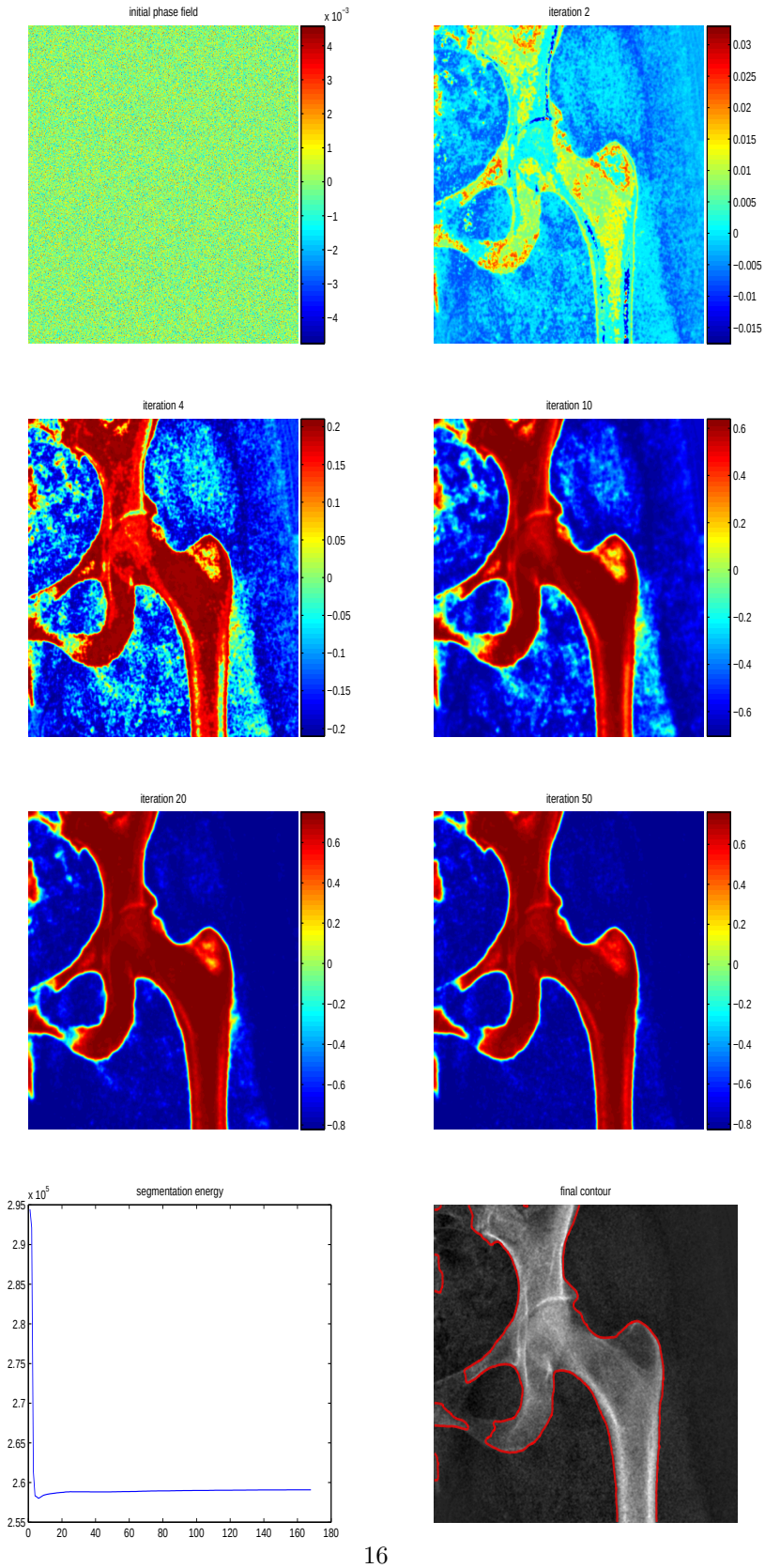

Figure 4: Segmentation of the femur image using the entropy descriptor, a random initialization and algorithm 1. Last row, left: variations of the energy as a function of the number of iterations.

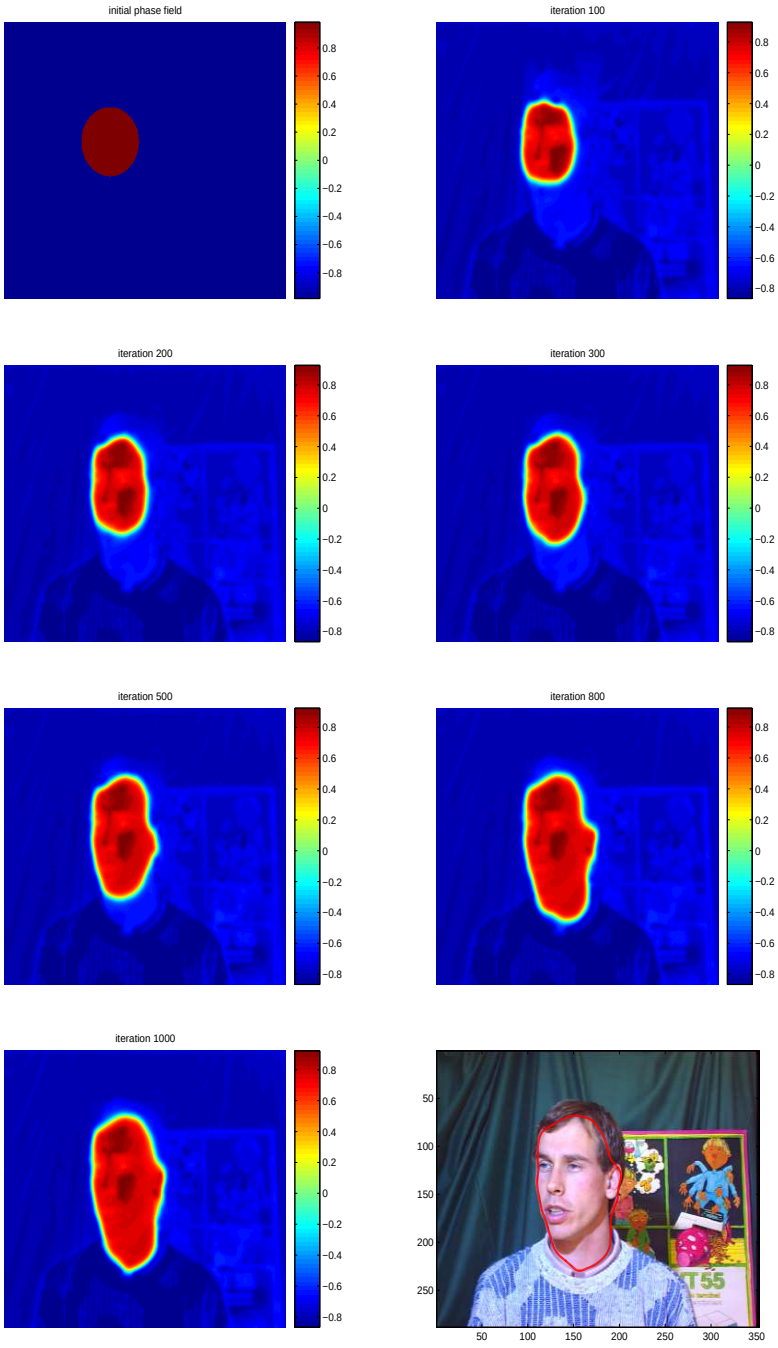

Figure 5: Segmentation of the it Erik image using the entropy descriptor, an initial contour and algorithm 1.

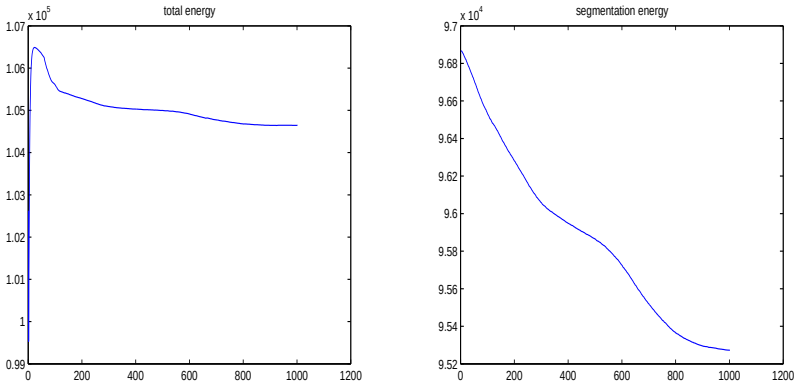

Figure 6: Variations of total energy (left) and segmentation energy (right) for the experiment of Fig. 5.

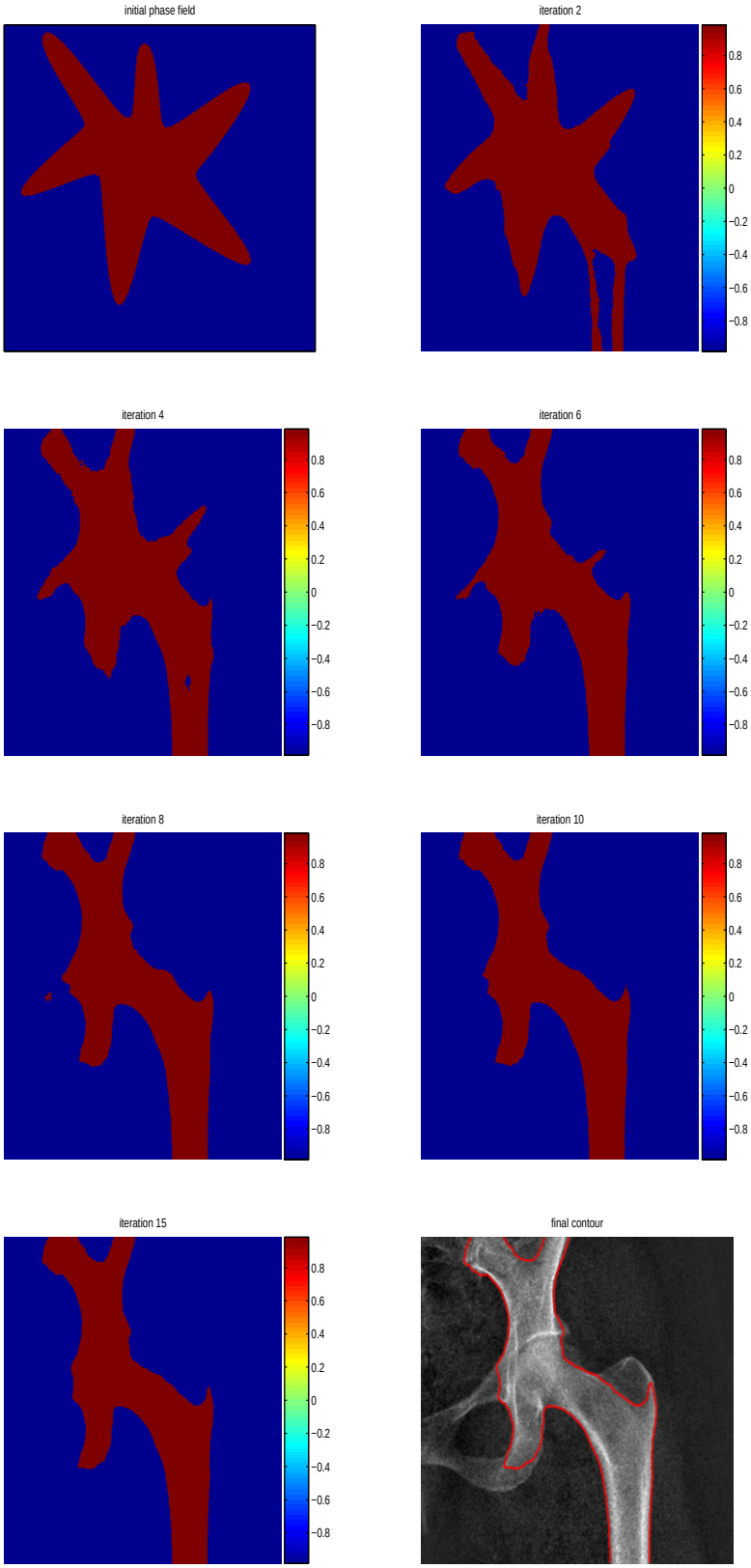

Figure 7: Segmentation of the femur image using the mean descriptor, an initial contour and algorithm 2.

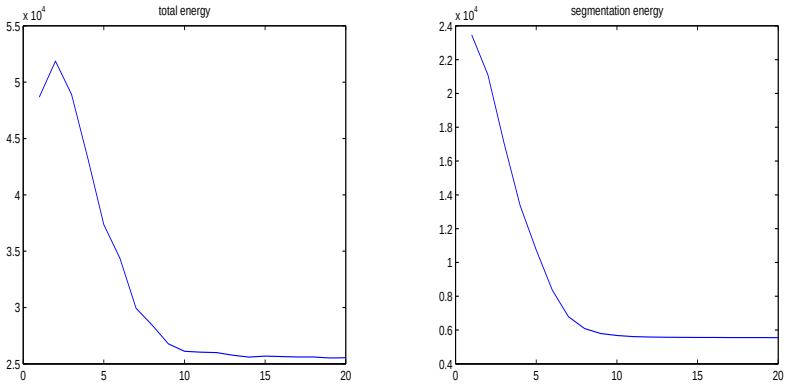

Figure 8: Variations of total energy (left) and segmentation energy (right) for the segmentation of the femur image using the mean descriptor, algorithm 2 and an initial contour (Fig. 7).

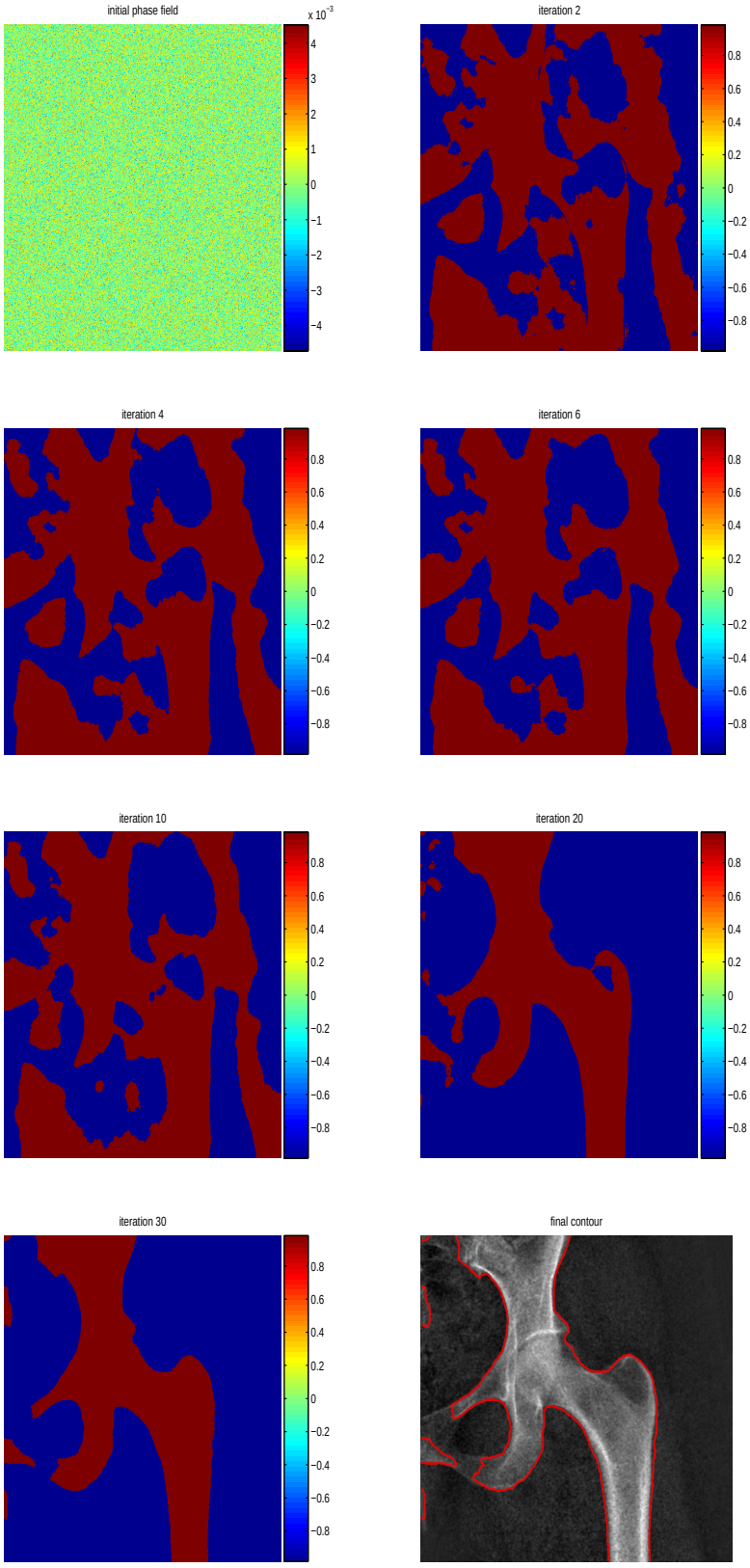

Figure 9: Segmentation of the femur image using the entropy descriptor, a random initialization and algorithm 2.

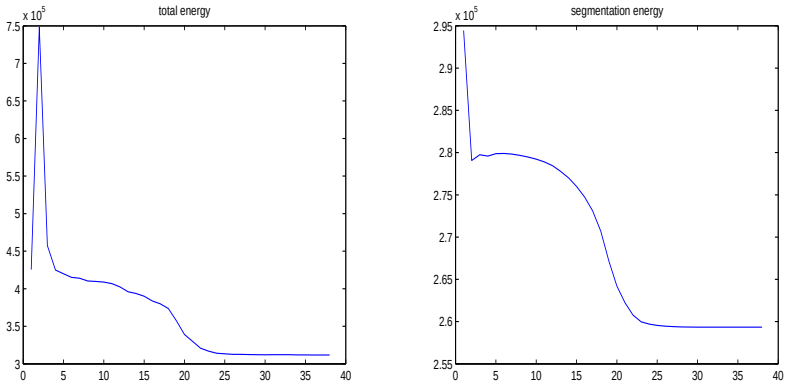

Figure 10: Variations of total energy (left) and segmentation energy (right) for the experiment of Fig. 9.

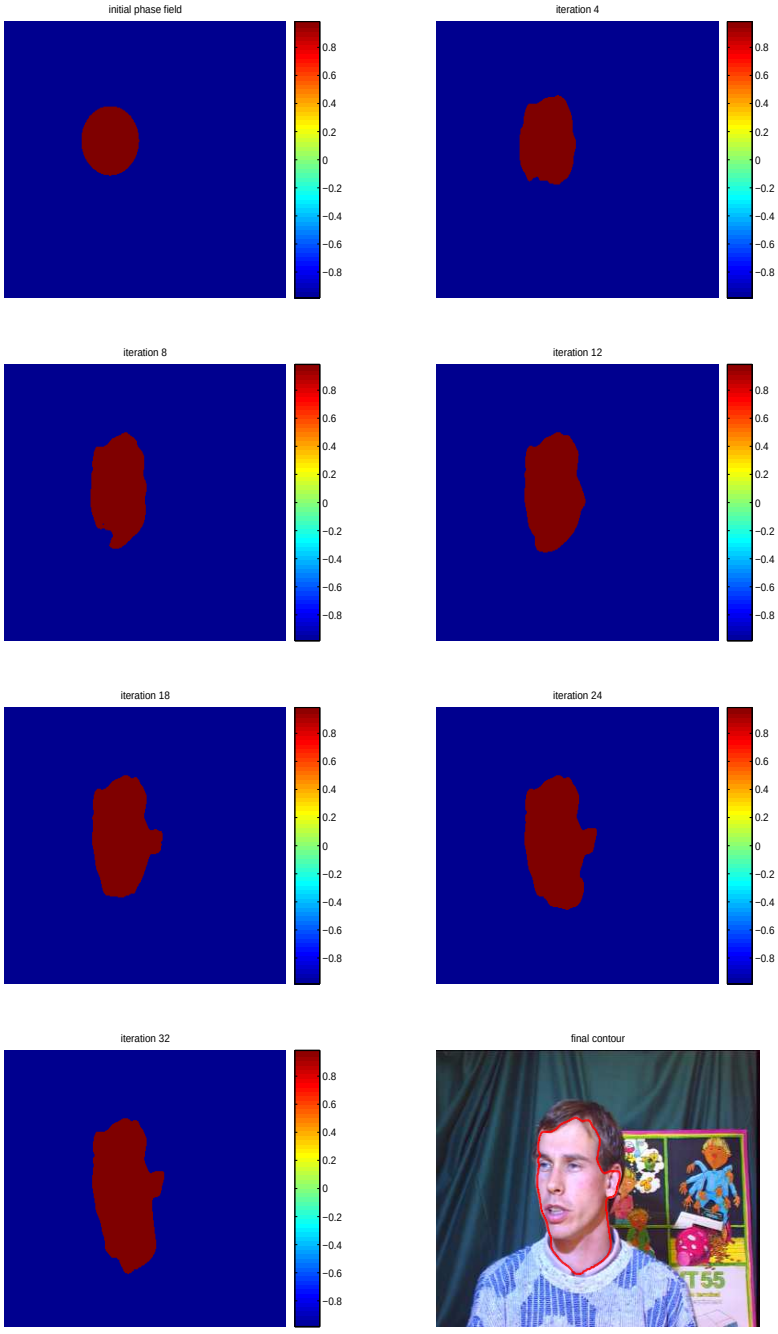

Figure 11: Segmentation of the *Erik* image using the entropy descriptor, an initial contour and algorithm 2.

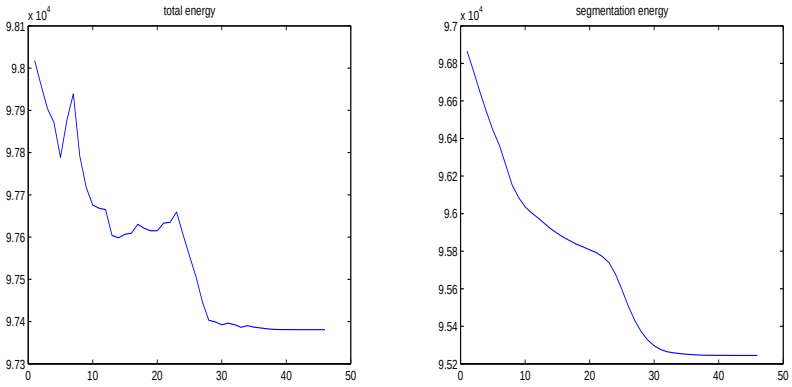

Figure 12: Variations of total energy (left) and segmentation energy (right) for the experiment of Fig. 11.

References

[1] S. Allen and J. Cahn. A microscopic theory for antiphase boundary motion and its application to domain coarsening. *Acta Metall.*, 27:1084–1095, 1979.

[2] G. Aubert, J.-F. Aujol, and L. Blanc-Féraud. Detecting codimension-two objects in an image with Ginzburg-Landau models. *International Journal of Computer Vision*, 65(1-2):29–42, 2005.

[3] G. Aubert, M. Barlaud, O Faugeras, and S. Jehan-Besson. Image segmentation using active contours: Calculus of variations or shape gradients. *SIAM J. Appli. Math.*, 63(6):2128–2154, 2003.

[4] T. F. Chan and L. A. Vese. Active contours without edges. *IEEE Transactions on Image Processing*, 10(2):266–277, 2001.

[5] E. Debreuve, M. Barlaud, G. Aubert, I. Laurette, and J. Darcourt. Space-time segmentation using level set active contours applied to myocardial gated SPECT. *IEEE Transactions on Medical Imaging*, 20(7):643–659, 2001.

[6] S Esedoglu and Y.-H. R. Tsai. Threshold dynamics for the piecewise constant Mumford-Shah functional. *Journal of Computational Physics*, 211(1):367–384, 2006.

[7] L.C. Evans and J. Spruck. Motion of level sets by mean curvature. *J. Diff. Geom.*, 33:635–681, 1991.

[8] P.C. Fife. *Dynamics of Internal Layers and Diffuse Interfaces.* SIAM, 1988.

[9] P.C. Fife and O. Penrose. Interfacial dynamics for thermodynamically consistent phase-field models with nonconserved order parameter. *Elec. J. Diff. Equ.*, 1995(16):1–49, 1995.

[10] J. Gomes and O. Faugeras. Reconciling distance functions and level sets. *J. Visual Com. and Image Representation*, 11:209–223, 2000.

[11] H. Grossauer and 0 Scherzer. Using the complex ginzburg-landau equation for digital inpainting in 2D and 3D. In *Proc. Scale Space*, volume 2695 of LNCS, pages 225–236, Springer, 2003.

[12] A. Herbulot, S. Jehan-Besson, M. Barlaud, and G. Aubert. Shape gradient for image segmentation using information theory. *Proceedings of IEEE International Conference on Acoustics, Speech, and Signal Processing (ICASSP)*, 3:21–24, Canada, May 2004.

[13] A. Herbulot, S. Jehan-Besson, S. Duffner, M. Barlaud, and G. Aubert. Segmentation of vectorial image features using shape gradients and information measures. *??*, ??:??, 2006.

[14] S. Jehan-Besson, A. Herbulot, M. Barlaud, and G. Aubert. *Shape Gradient for Image and Video Segmentation.* Mathematical Models in Computer Vision: The Handbook. Springer, 2005.

[15] M. Kass, A. Witkin, and D. Terzopoulos. Snakes: Active contour models. *International Journal of Computer Vision*, 1(4):321–331, 1988.

[16] J. Kim, J Fisher III, A. Yezzi, M. Cetin, and A.S. Willsky. Nonparametric methods for image segmentation using information theory and curve evolution. In *Proc. International conference on Image Processing*, 2002.

[17] C. Li, C. Xu, C. Gui, and M.D. Fox. Level set evolution without reinitialization: A new variational formulation. In *Proc. IEEE International Conference on Computer Vision and Pattern Recognition CVPR*, pages 430–436, San Diego, USA, 2005.

[18] Barry Merriman, James K. Bence, and Stanley J. Osher. Motion of multiple junctions: A level set approach. *Journal of Computational Physics*, 112(2):334–363, 1994.

[19] S Osher and J.A. Sethian. Fronts propagating with curvature-dependent speed: Algorithms based on Hamilton-Jacobi formulation. *Journal of Computational Physics*, 79:12–49, 1988.

[20] F. Precioso, M. Barlaud, T. Blu, and Unser M. Robust real-time segmentation of images and videos using a smoothing-spline snake-based algorithm. *IEEE Trans. on Image Processing*, 2005.

[21] M. Rochery, I.H. Jermyn, and J. Zerubia. Phase field models and higher-order active contours. In *Proc. IEEE International Conference on Computer Vision (ICCV)*, Beijing, China, october 2005.

[22] J. Rubinstein, P. Sternberg, and J.B. Keller. Fast reaction, slow diffusion and curve shortening. *SIAM J. Appli. Math.*, 49:116–133, 1989.

[23] C. Samson, L. Blanc-Fraud, G. Aubert, and J. Zerubia. Simultaneous image classification and restoration using a variational approach. In *Proc. IEEE Computer Vision and Pattern Recognition (CVPR)*, Fort Collins, Colorado, USA, june 1999.

[24] J.A. Sethian. *Level set methods and fast marching methods.* Cambridge Monographs on Applied and Computational Methematics. Cambridge University Press, 1999.

[25] J. Shen. Γ-*Convergence Approximation to Piecewise Constant Mumford-Shah Segmentation*, volume 3708 of *Lecture Notes in Computer Science*, pages 499–506. J. Blanc-Talon et al. (Eds), 2005.